Crack growth simulation in heterogeneous material by S-FEM and comparison with experiments

Masanori Kikuchi
Tokyo University of Science, 2641 Yamazaki, Noda, Chiba, 278-8510, Japan
kik@rs.noda.tus.ac.jp

Yoshitaka Wada
3-4-1, Kowakae, Higashi-Oosaka, Oosaka, 577-0818, Japan
wada@mech.kindai.ac.jp

Yulong Li
Northwestern Polytechnical University, 127 Youyi Xilu, Xian 710072 Shaanxi, P.R.China
liyulong@nwpu.edu.cn

ABSTRACT. Fully automatic fatigue crack growth simulation system is developed using S-version FEM (S-FEM). This system is extended to fracture in heterogeneous material. In the heterogeneous material, crack tip stress field becomes mixed mode condition, and crack growth path is affected by inhomogeneous materials and mixed mode conditions. Stress Intensity Factors (SIF) in mixed mode condition are evaluated using Virtual Crack Closure Method (VCCM). Criteria for crack growth amount and crack growth path are used based on these SIFs, and growing crack configurations are obtained.
Three crack growth problems are simulated. One is crack growth in bi-materila made of CFRP plate and Aluminum alloy. Initial crack is located in CFRP plate, and grows toward Aluminum alloy. Crack growing direction changes and results are compared with experimental one. Second problem is crack growth in bi-material made of PMMA and Aluminum alloy. Initial crack is located in PMMA plate and parallel to phase boundary. By cahnging loading conditions, several cases are simulated and compared with experimental ones. In the experiment, crack grows into pahse boundary and grow along it. This case is simulated precisely, and the effect of pahse boundary is discussed. Last case is Stress Corrosion Cracking (SCC) at Hot-Leg Safe-End of Pressurized Water Rreactor. This location is made of many kinds of steels by welding. In some steel, SCC does not occur and in other steel, SCC is accelerated. As a result, small surface crack grows in complicated manner.

KEYWORDS. Heterogeneous Material; S-FEM; Fatigue; SCC; VCCM.

INTRODUCTION

Fatigue crack growth is important problem for the integrity of structures. To avoid catastrophic accident, predictions of crack growth path and fatigue life are key technologies. As fatigue crack growth occurs in complicated structures, these predictions have met serious difficulties. FEM is usually used for these predictions,

but re-meshing process is needed for modeling of growing crack configurations, it has been a bottleneck for the application of FEM to fatigue crack growth problems, especially in three-dimensional field.
Recently, several new techniques have been developed to overcome these difficulties. Element Free Galerkin Method [1], X-FEM [2] and Superposion-FEM(S-FEM[3]) have been developed to make re-meshing processes easy, and predict complicated crack paths. Authors have developed fully automatic fatigue crack growth simulation system[4], and applied it to three-dimensional surface crack problem, interaction evaluation of multiple surface cracks[5] and evaluation of crack closure effect of surface crack[6]. This system is developed for residual stress field problem, and Stress Corrosion Cracking process is simulated [7]. Residual stress field is generated by welding, and evaluation of crack growth in Heat Affected Zone (HAZ) is another important problem. In HAZ, grain size is different from other area, and mechanical properties are different from those of base metals. For the evaluation of SCC in such areas, changes of material properties should be considered. In S-FEM, local mesh is re-meshed for each step of crack growth, and local area changes its' shape in each step. It seems difficult to change material properties of local mesh following the change of local mesh shape. In this paper, this problem is solved, and crack growth simulation system in heterogeneous material is developed. In the following, this new method is explained briefly, and example problem is simulated and compared with previous works to verify this method. Several practical problems are simulated and effect of existence of interface and changes of material properties are studied and discussed.

APPLICATION OF S-FEM TO HETEROGENEOUS MATERIAL.

S-FEM is originally proposed by J. Fish [3]. As shown in Fig.1, a structure with a crack is modeled by global mesh and local mesh. Global area, Ω^G, does not include a crack, and course mesh is used for the modeling of global area. A crack is modeled in local area, Ω^L, using fine mesh around crack tip. Local area is superimposed on global area and full model is made. In each area, displacement function is defined independently. In overlapped area, displacement is expressed by the summation of displacement of each area. To keep the continuity at the boundary between global and local area, Γ^{GL}, displacement of local area is assumed to be zero as shown in the following equation.

$$u_i = \begin{cases} u_i^G & i \in \Omega^G - \Omega^L \\ u_i^G + u_i^L & i \in \Omega^L \\ u_i^L = 0 & i \in \Gamma^{GL} \end{cases} \tag{1}$$

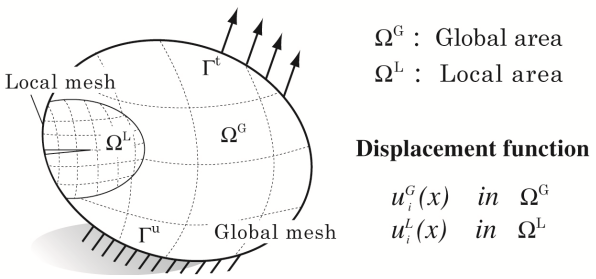

Figure 1: Concept of S-FEM.

The derivatives of displacements can be written in the same way. These displacement functions are applied to virtual work principle, as shown in Eq. (2), and .the final matrix form of S-FEM is obtained as shown in Eq. (3)

$$\begin{aligned} &\int_{\Omega^G} \delta u_{i,j}^G D_{ijkl} u_{k,l}^G d\Omega + \int_{\Omega^L} \delta u_{i,j}^G D_{ijkl} u_{k,l}^L d\Omega \\ &+ \int_{\Omega^L} \delta u_{i,j}^L D_{ijkl} u_{k,l}^G d\Omega + \int_{\Omega^L} \delta u_{i,j}^L D_{ijkl} u_{k,l}^L d\Omega = \int_{\Gamma^t} \delta u_i^G t_i d\Gamma^{tG} \end{aligned} \tag{2}$$

$$\begin{bmatrix} [K^{GG}] & [K^{GL}] \\ [K^{LG}] & [K^{LL}] \end{bmatrix} \begin{Bmatrix} \{u^G\} \\ \{u^L\} \end{Bmatrix} = \begin{Bmatrix} \{t^G\} \\ 0 \end{Bmatrix} \tag{3}$$

where

$$\left[K^{GG}\right]=\int_{\Omega^G}\left[B^G\right]^T\left[D^{GG}\right]\left[B^G\right]d\Omega \qquad \left[K^{GL}\right]=\int_{\Omega^L}\left[B^G\right]^T\left[D^{LL}\right]\left[B^L\right]d\Omega \tag{4}$$

$$\left[K^{LL}\right]=\int_{\Omega^L}\left[B^L\right]^T\left[D^{LL}\right]\left[B^L\right]d\Omega$$

$\left[B^G\right]$ and $\left[B^L\right]$ are displacement- strain matirces defined in global and local area, respectively. $\left[D^{GG}\right]$ and $\left[D^{LL}\right]$ are stress-strain matices which are described using young's modulus and poisson's ratio. These are material constants which may change in heterogenous material in each material.

In Eq. (3), $\left[K^{LG}\right]^T=\left[K^{GL}\right]^T$, and the stiffness matrix is symmetric. $\left[K^{GL}\right]$ expresses the relationship between local and global areas. By calculating this term with high accuracy, accurate FEM results are obtained. By solving Eq.(3), both displacement fields of local and global areas are obtained simultaneously. The detail of the theory was presented in the literature of one of the author [8].

This method is applied to crack growth in heterogeneous material. As shown in Fig.2, global model is made of two materials, and it is easy to define phase bounday in global model. Material properties are different from each other in material 1 and 2. But in local area, it is seen that it is difficult to arrange mesh in local area along phase boundary of global model. Local mesh is overlapped on global mesh. $\left[K^{GL}\right]$ and $\left[K^{LL}\right]$ are calculated by eq.(4), and $\left[D^{LL}\right]$, material properties in each material, are needed for these calculations. As shown in Fig.2, integrations are conducted using Gaussian numerical integration method in each local element, and material properties at these Gaussian points are needed for integration. In S-FEM analysis, all Gaussian points in local elements belong to some global element. Then, material properties of each Gaussian point is same as those of global element in which Gaussian point is located. For this meaning, local mesh needs not to have material properties, and it becomes easy to calculate eqs.(4) using material properties of global element. By this method, it becomes possible to apply S-FEM methodology to crack growth simulation in heterogeneous material.

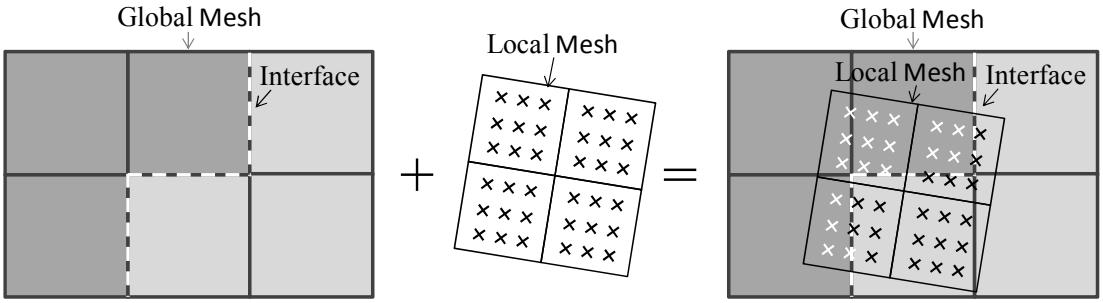

Figure 2: Global mesh and local mesh in heterogeneous material.

CRACK GROWTH IN BI-MATERIAL OF CFRP AND ALUMINUM ALLOY

Fig. 3 shows test specimen made of aluminum alloy, A2017 and CFRP. As shown in Fig. 4, fiber orientation of CFRP plate is 90 degree to loading direction. Initial notch is introduced in CFRP plate and grows toward to A2017. Phase boundary of two material is inclined about 80 degree to horizontal axis. Tensile load is subjected along x axis in Fig. 4. Mechanical properties of these two materials are shown in Tab. 1. Young's modulus of A2017 is much larger than that of CFRP. Fig. 5(a) shows experimental result. Initial crack grows toward to phase boundary, and it changes growing direction a little to upper ward. This is the effect of mismatch of mechanical properties between two materials. As the Young's modulus of A2017 is larger than that of CFRP, crack prefers to stay in CFRP side. Finally it reaches to the phase boundary, and separation occurred between two materials. Fig. 5 (b) shows result of numerical simulation. In this paper, crack growing direction is determined using the Maximum Tangential Stress (MTS) criterion [9], which determines the crack growth direction, θ , to satisfy the following equation,

$$\frac{\partial \sigma_\theta}{\partial \theta} = K_I \sin\theta + K_{II}\left(3\cos\theta - 1\right) = 0 \tag{5}$$

where K_I and K_{II} are Stress Intensity Factors (SIF) in mode I and II, respectively. Fig. 5 (c) shows overlapped result of experiment and numerical simulation. It is noticed that both results agree very well. It also means that MTS criterion is available to predict crack growing direction under mixed mode loading condition.

Figure 3: Specimen of composite material (CFRP & A2017).

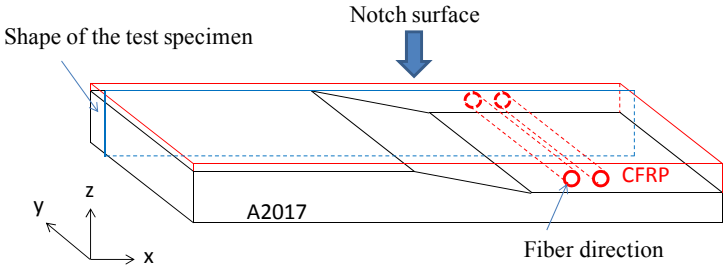

Figure 4: Overview of specimen and direction of fiber.

Material constant	Young's modulus E (GPa)	Poisson's ratio ν
A2017	70.6	0.30
CFRP (perpendicular direction of fiber	9.53	0.49

Table 1: Material constants.

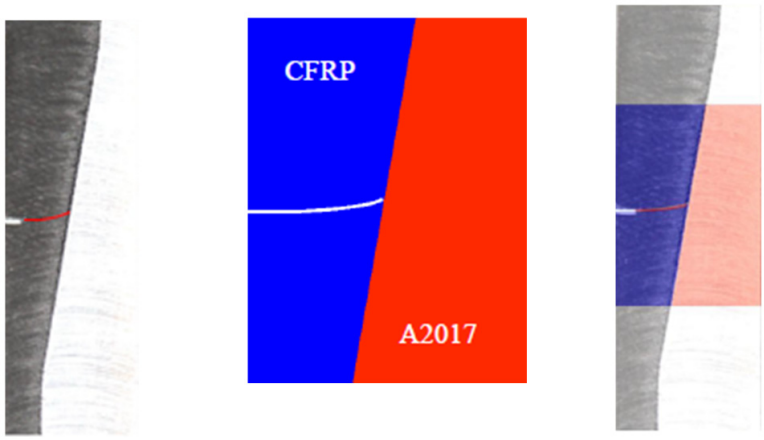

(a) Experimental result. (b) Numerical simulation (c) Overlapping of both results.

Figure 5: Comparison of crack path in bi-material.

CRACK GROWTH IN A BI-MATERIAL OF PMMA AND A6061

Lee and Krishnaswamy [10] conducted experiment of crack growth in bi-material made of PMMA and aluminum alloy Al6061. As shown in Fig.6, PMMA and Al6061 were pasted, and initial crack is introduced in PMMA. Three loading conditions are tested, as shown in Fig. 6 (a)-(c), and crack growing paths are obtained. In case (a),

nearly symmetrical loading condition is subjected. In case (b), loading condition is not symmetric, and supporting load in PMMA is near to initial crack. In case (c), supporting load becomes much nearer to the initial crack. The distance between initial crack and phase boundary is 10mm in Case1 and Case 3, and 16mm in Case 2. In all cases, stress field at initial crack tip becomes under mixed mode loading condition, and crack grows by changing the growing direction. Table 2 shows material constants of two materials. In this case, Young's modulus of PMMA is much smaller than that of aluminum alloy.

Experimental results are shown in Fig. 7 (a)-(c) with those of numerical simulation where experimental results are shown by yellow lines, and numerical results are expressed by red line. In case 1, crack grows toward inside of PMMA and goes far from phase boundary. Numerical simulation well predicts the crack growth path, and agrees very well with experimental one. In case 2, crack grows nearly straight forward in numerical simulation and experiment. In this case agreement of numerical prediction and experiment is well. In case 3, difference between experiment and numerical simulation becomes clear. By the experiment, crack grows into the phase boundary and grows along the phase boundary. But numerical simulation predicts that crack grows once nearer to the phase boundary, but after some amount of crack growth, it goes far from the phase boundary. This difference is due to the numerical model in which phase boundary is not modelled correctly. Numerical model assumes that two materials are bonded tightly and there is no phase boundary thickness. But in the real structure, phase boundary has some small thickness and has its' own strength.

Then phase boundary is modelled in S-FEM simulation. Fig. 8 shows mesh pattern around phase boundary. The thickness of the phase boundary is assumed to be 0.5mm, and three layered finite element mesh is used. Material constants of the phase boundary are also shown in Tab. 2. It is assumed that phase boundary has very small stiffness comparing with other materials. It is because two materials are bonded using some bond, and it is reasonable to assume that it has very low stiffness. Numerical result is shown in Fig. 9 (a). By assuming phase boundary layer, crack grows into the phase boundary and grows along it. It is similar to experimental result, but path does not agree completely. This may be due to the phase boundary model. In this simulation, the thickness of phase boundary is assumed to be 0.5mm, which may be much larger than the real structure. Also, material constants in the phase boundary are assumed to be very small value, without any verification. By studying in detail on the effects of phase boundary thickness and material constants, better phase boundary model may be proposed in future. Fig. 9 (b) shows detailed crack path in the phase boundary. It grows in the phase boundary layer in zig-zag manner. As the crack grows in the phase boundary, and does not grow along the border line between different materials, it is easy to evaluate stress intensity factors by the conventional VCCM method [11].

In many composite materials, for example, CFRP, crack growth along phase boundary is observed. The strength of phase boundary is key parameter for the discussion on the strength of composite material. Experimental studies have been done by many authors [12-14], but it has been very difficult to discuss this problem based on numerical simulation. Through these simulations, it is shown that crack growth process along phase boundary becomes possible, if the phase boundary is properly modelled.

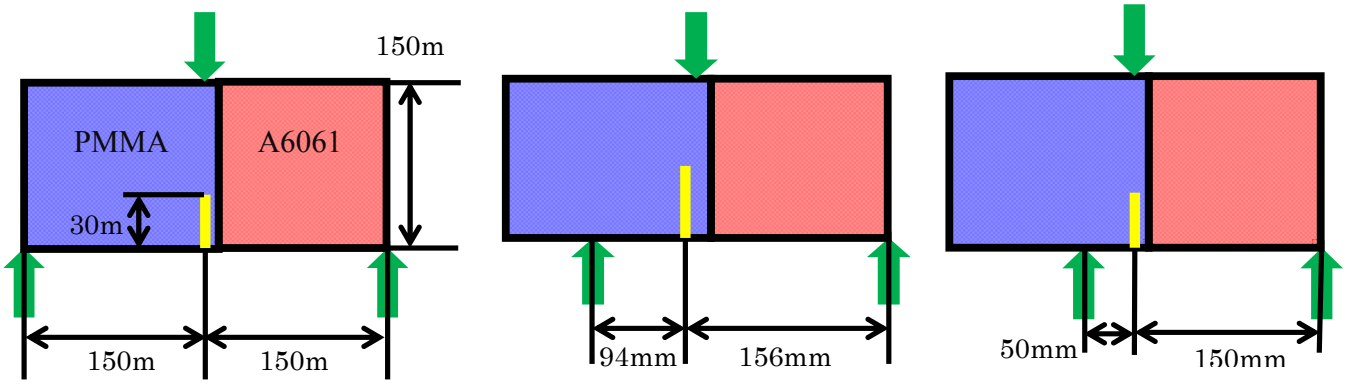

(a) Case 1 (b) Case 2 (c) Case 3

Figure 6: Initial carack location and loading conditions of bi-material of PMMA and A6061.

	PMMA	A6061	Phase boundary
E [GPa]	3.24	69	0.15
ν	0.35	0.3	0.35

Table 2: Material constants.

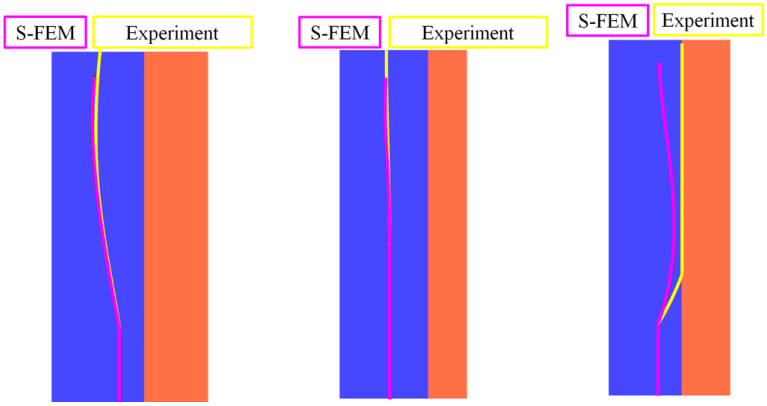

(a) Case 1 (b) Case 2 (c) Case 3

Figure 7: Crack growth path in experiment and numeircal simulation.

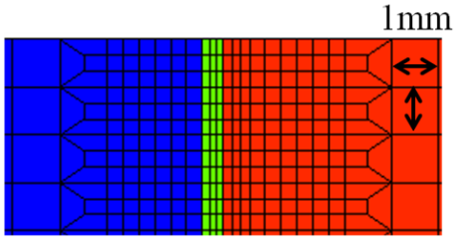

Figure 8: FEM model of phase bourdary.

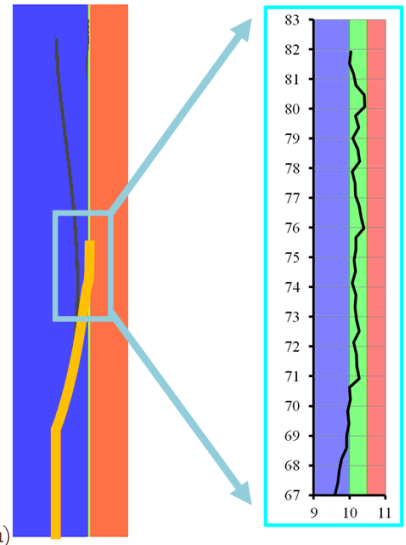

(a) (b)

Figure 9: Crack growth in the phase boudary. (a) Crack path (b) Detail in phase boundary.

STRESS CORROSION CRACKING IN HOT LEG OF NUCLEAR PLANT DUE TO WELDING THERMAL STRESS

Stress corrosion cracking (SCC) frequently occurs in nuclear plant by welding thermal residual stress. Fig. 10 shows half of hot leg of a pipe at nuclear pressure vessel. It is welded to pressure vessel using several kinds of welding metals. Fig. 10 shows circumferentioal residual stress field by welding, which is obtained by numerical welding simulation. Residual stress field is generated in the cross section of hot leg, which triggers the crack initiation and growth by stress corrosion. Detailed cross section of this hot leg is shown in Fig.11. Hot leg is made of three materials. They are low carbon steel, stainless steel and Ni-based alloy. Material constants of them are shown in Tab. 3. Crack growth rate by stress corrosion is expressed by Eq. (6), where α and β are material constants [15], and are shown in Tab. 2. SCC does not occur in law carbon steel and stainless steel, and occurs only in Ni-based alloy.

$$da / dt = \alpha \left(K_{eq} \right)^{\beta} \tag{6}$$

Initial crack is assumed in Ni-based alloy, in green area in Fig.11, and crack growth simulation is conducted. Figs. 12 (a)-(e) show crack growing processes. Initial crack is located inside of hot leg pipe, where residual hoop stress is very large. This initial carck grows gradually and goes near to phase boundary between low carbon steel and stainless steel. It terminates at the phase boundary, and crack continues growing inside Ni-based alloy. After 30 years, crack grows nearly

half of the plate thickness. Fig. 14 shows change of crack depth and crack length along inner sursface with time (year). In the first several years, crack grows very rapidly, but growth rate decreases in low residual stress area. After 27 years, crack depth increases again very fast. If the crack depth exceeds 75% of plate thickness, this crack is treated to be fixed immediately. This crack reaches to this limit depth after 27 years, as shown in Fig.13. It is enoughly long time for the usual operation of nuclear power plant. By using this method, similar estimation of SCC process is possible. It enables to evaluate correctly the integrity of nuclear components.

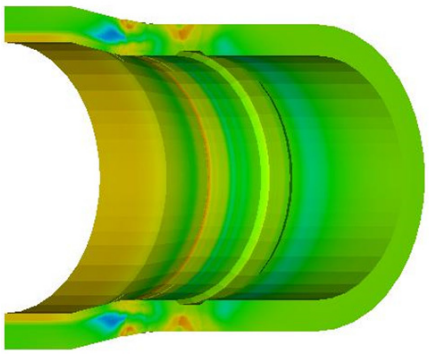

Figure 10: Residual stress distribution in Hot Leg.

Figure 11: Cross section of hot leg and materials.

Material	E[GPa]	ν	a	β
Low Carbon Steel	176.0	0.3	0.0	1.00
Stainless Steel	174.5	**0.3**	0.0	1.00
Ni-based Alloy	198.3	**0.3**	6.73×10^{-14}	2.42

Table 3: Material constants of hot leg materials.

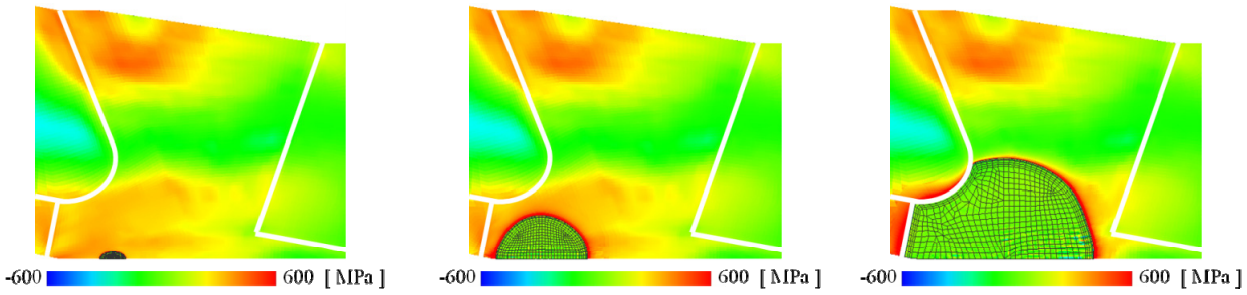

(a) Initial crack (0 year). (b) 1.95 years. (c) 15.4 years.

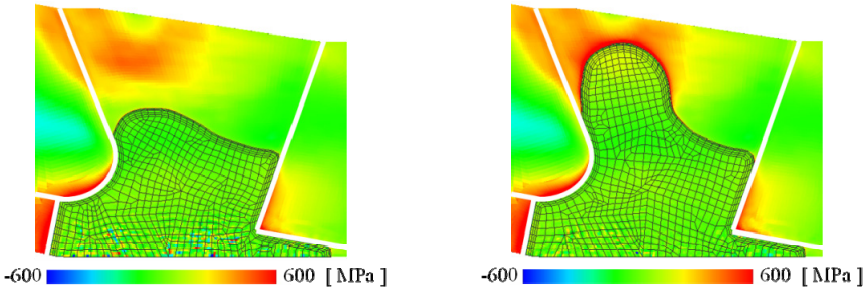

(d) 22.8 years. (e) 30.2 years.

Figure 12: SCC growing process in the hot leg.

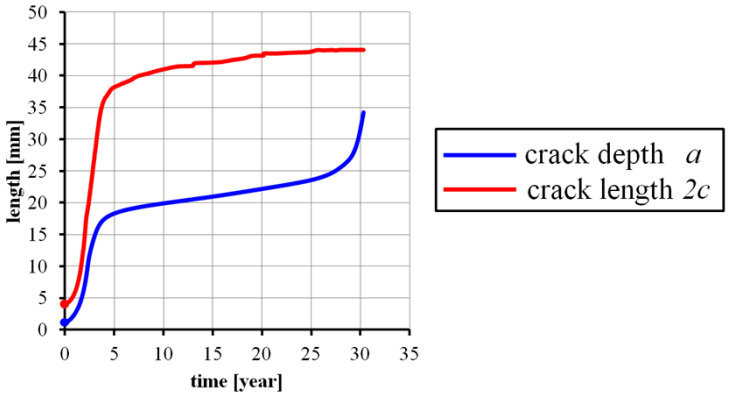

Figure 13: Crack growth rates.

SUMMARY

Three crack growth problems in heterogenous material are simulated using S-version FEM. In two cases, results are compared with experimental ones, and good agreements are obtained. It is verified that S-FEM is powerful tool for these compicated problems. It is also shows that fracture process along phase boundary is also simulated by this method. By careful modeling of phase boundary layer, realistic fracture process in CFRP plate becomes possible.

REFERENCES

[1] Belytchko, T,. Lu, Y.Y., Gu, L.,Element Free Galerkin Method, International Journal for Numerical Methods in Engineering, 37 (1994) 229-256.
[2] Belytschko, T., Black, T., Elastic crack growth in finite elements with minimal remeshing, International Journal for Numerical Methods in Engineering, 45 (1999) 601-620.
[3] Fish, J., Markolefas, S., Guttal, R., Nayak, P., On adaptive multilevel superposition of finite element meshes, Applied Numerical Mathematics, 14 (1994) 135-164.
[4] Kikuchi, M., Wada, Y., Takahashi, M., Li, Y., Fatigue Crack Growth Simulation using S-version FEM, Proc. ASME PVP2008, PVP2008-61900.
[5] Kikuchi, M., Interacation Evaluation between Two Surface Cracks by Fatigue, Proc. ASME PVP2009, PVP2009-77073.
[6] Kikuchi, M., Maigefeireti, M., Sano, H., Closure Effect on Interaction of Two Surface Cracks under Cyclic Bending, Proc. ASME PVP2010, PVP2010-25241.
[7] Kikuchi, M., Wada, Y., Shimizu, Y., Li, Y., Crack growth analysis in a weld-heat-affected zone using S-version FEM, Int. J. PVP, 90-91 (2012) 2-8.
[8] Okada, H., Endo, S., Kikuchi, M., On Fracture Analysis using an Element Overlay Technique, Engng. Fracture Mech., 72 (2005) 773-789.
[9] Paris, P.C., Erdogan, F., A critical analysis of crack propagation of laws, Trans. ASME Ser. D, (1963) 528-533.
[10] Lee, H., Krishnaswamy, S., Quasi-static propagation of subinterfacial cracks, ASME Journal of Applied Mechanics, 67(3) (2000) 444-452.
[11] Rybicki, E. F., Kaninen, M.F., A Finite Element Calculation of Stress Intensity Factors by a Modified Crack Closure Integral, Engng. Fracture Mech., 9 (1977) 931.
[12] Konur, O., Matthews, F.L., Effect of the properties of the constituents on the fatigue performance of composites: a review, Composites, 20-4 (1989) 317-328.
[13] Wu, C.M.L., Thermal and mechanical fatigue analysis of CFRP laminates, Composite Structures, 25 (1993) 339-344.
[14] Kawai, M., Morishita, M., Fuzi, K., Sakurai, T., Kemmochi, K., Effect of matrix ductility and progressive damage on fatigue strength of unnotched and notched carbon fiber plain woven roving fabric laminates, Composites: Part A, 27A (1996) 493-502.
[15] JSME S Nal-2004, Codes for Nuclear Power Generation Facilities, (2004), (In Japanese).